

## SURFACE MODIFICATION OF RHODIUM-DOPED STRONTIUM TITANATE BY ADSORPTION OF COBALT CLATHROCHELATES FOR WATER PHOTO-DISSOCIATION

Villagra A.<sup>1</sup>, Ranjbari A.<sup>1</sup>, Kudo A.<sup>2</sup>, Millet P.<sup>1</sup>

<sup>1</sup> Université Paris-Sud, ICMMO, 91405 Orsay cedex France

<sup>2</sup> Tokyo University of Science, 1-3 Kagurazaka, Tokyo 162-8601, Japan

E-mail: [pierre.millet@u-psud.fr](mailto:pierre.millet@u-psud.fr)

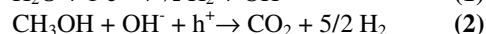
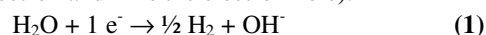
### ABSTRACT

Photo-electrochemical water splitting was first put into evidence and investigated by Honda and Fujishima in 1972. Since then, a large variety of semi-conducting materials, that can absorb either UV or visible light and that have appropriate band edge features, have been synthesized and characterized. The purpose of this communication is to report on the photo-dissociation of water using Strontium Titanate as photo-material. Rhodium doping has been used to modify the band structure of the perovskite and extend its light absorption range towards visible light. Methanol has been used as sacrificial agent (the overall reaction under investigation is the endergonic methanol steam photo-reforming reaction). Experiments have been performed at close-to-room temperature under visible light irradiation. The rates of water photo-reduction into hydrogen and methanol oxidation into carbon dioxide have been determined by gas chromatography analysis. Negligible amounts of hydrogen and carbon dioxide were found to form on pristine samples. However, the kinetics of the reaction was found to increase by surface deposition of metallic platinum nano-particles that act as surface co-catalyst for either water reduction into hydrogen or methanol oxidation reaction, or both. This is an indication that charge transfer processes at the semi-conductor/electrolyte interface can be considered (at least partly) as rate-determining. In addition to hydrogen and carbon dioxide, other oxidation by-products have been detected but not carbon monoxide, a poison that could potentially adsorb on Pt surfaces and inhibit reaction sites. In order to gain a better understanding of co-catalytic phenomena, we also investigated the co-catalytic effect of cobalt-clathrochelates that are known to be efficient electrocatalysts for the hydrogen evolution reaction but poor electrocatalysts for methanol oxidation. It is found that the presence of cobalt complexes has also a positive catalytic effect on the kinetics of the reaction but a loss of performance has been observed with time. This can be attributed to either inhibition of methanol oxidation or surface contamination by photo-degradation products.

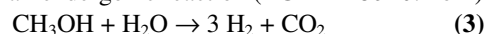
### INTRODUCTION

A photo-electrochemical cell (PEC) is basically a galvanic chain that uses sunlight as power source to perform endergonic transformations such as water dissociation. Photo-electrodes made of semi-conducting materials are used to transform photons into electron-hole charge carriers that are then separated and used to perform redox transformations at semiconductor-electrolyte interfaces. A PEC contains either a photoanode, or a photocathode or even both [1]. Photo-electrochemical water splitting was first put into evidence and investigated by Honda and Fujishima in 1972 [2]. At that time, UV-absorbing titanium dioxide was used as photo-anode material. Since then, significant progress has been made and a large variety of n-type and p-type semi-conductors that can absorb visible light and provoke water photo-dissociation have been synthesized and characterized [3], yielding a better understanding of elemental processes in such systems.

Strontium titanate SrTiO<sub>3</sub> is an n-type oxide semi-conductor with a large ( $\approx 3.2$  eV) band gap. Rhodium doping is used to modify the band structure of the titanate (band gap  $\approx 2.3$  eV), thus extending the light absorption range toward the visible light. It also confers p-type semi-conducting properties to the material [4]. But the resulting driving force is not sufficient to split water and a sacrificial agent is required. When methanol is used in the experiments, the overall reaction under investigation is the endergonic methanol steam photo-reforming reaction. Under neutral pH conditions, half redox reactions are (where e<sup>-</sup> is the electron and h<sup>+</sup> is the electron hole):



The overall endergonic reaction ( $\Delta G = + 180 \text{ kJ.mol}^{-1}$ ) is:



Whereas the photo-electrochemical properties of SrTiO<sub>3</sub>:Rh(1wt.%) have already been reported in the literature, the objective of the work reported here was to investigate the role of surface co-catalysts because it is known that charge transfer in such systems is rate-determining. Therefore, a better

understanding of surface co-catalysis is expected to open the way to more efficient PECs. In spite of its cost that would alleviate its implementation in systems of commercial interest, Pt is a good candidate for that purpose. It can potentially promote both water reduction into hydrogen and methanol oxidation into carbon dioxide. However, which of the two paths is the rate-determining step is still unclear. In addition, as in direct methanol fuel cells, methanol oxidation on platinum can lead to the formation of carbon monoxide, a poison that can potentially adsorb on Pt surfaces, inhibit reaction sites and degrade performances. Therefore selective co-catalysts are required. Molecular chemistry offers some interesting opportunities. For example, cobalt clathrochelates that are excellent hydrogen evolving catalysts [5] can be used for that purpose. Hence we report here on the photo-dissociation of water with methanol as sacrificial agent, using Rhodium-doped strontium titanate [4], surface modified by adsorption of either Pt nano-particles or cobalt clathrochelates [5].

## EXPERIMENTAL SECTION

### Rhodium-doped Strontium Titanate

The Rh-doped SrTiO<sub>3</sub> powder was synthesized through a solid state reaction. Starting materials (SrCO<sub>3</sub>, TiO<sub>2</sub>, and Rh<sub>2</sub>O<sub>3</sub>) were mixed with a small amount of methanol, in proportions corresponding to the stoichiometry of SrTi<sub>1-x</sub>M<sub>x</sub>O<sub>3</sub>. Then the mixture was calcined in air at 1373K for 10 h using an alumina crucible (purity: 99.7%). X-ray analysis was used to check the phase purity and crystallinity of the resulting material.

### Pt co-catalysts

Pt nano-particles of co-catalysts were deposited in situ at the surface of SrTiO<sub>3</sub> particles as follows. First, the SrTiO<sub>3</sub> particles were dispersed in water under vigorous stirring. Then, an aqueous solution of hexachloroplatinic acid was added to the solution under constant visible light illumination. H<sub>2</sub>PtCl<sub>6</sub> was spontaneously reduced at the surface of SrTiO<sub>3</sub> particles into Pt nano-particles by photo-reduction.

### Cobalt complex co-catalysts

The cobalt dimethyl tris-glyoximate co-catalyst has been synthesized starting from cobalt acetate and dimethyl glyoxime. Details about the synthesis are provided in Ref. [6]. The complex was loaded in situ by direct impregnation of the perovskite powder under constant stirring.

### Experimental setups, electrodes and gas analysis

Photocatalytic H<sub>2</sub> evolution experiments with Pt-SrTiO<sub>3</sub>:Rh(1 wt.%) from an aqueous methanol solution (10 vol %) was carried out in a closed gas circulation system [4]. The photocatalyst powder (0.3 g, 300 cm<sup>3</sup>, 1 mg/cm<sup>3</sup>) was dispersed with a magnetic stirrer in a reactant solution in the cell equipped with a top-window made of Pyrex. The undoped and Rh-doped SrTiO<sub>3</sub> photocatalyst electrodes used to record cyclic voltamograms were readily prepared by pasting SrTiO<sub>3</sub>:Rh powder on an indium tin oxide (ITO) transparent electrode followed by subsequent calcination. Photoelectrochemical

measurements were conducted using a conventional H-type cell and a potentiostat. The light source was a 300 W Xe lamp attached with cut-off filters to control the wavelength of the incident light. The amounts of evolved gases were determined using on-line gas chromatography (Shimadzu: GC-8A, MS-5A column, TCD, Ar carrier).

Experiments with cobalt co-catalyst have been performed in batch mode using the experimental set-up of figure 1. 15 mg of SrTiO<sub>3</sub>:Rh powder has been dispersed in 15 cm<sup>3</sup> and a water-methanol (10 vol.%) mixture under constant stirring. 10 mg of cobalt complex have been added. The amounts of evolved gases were determined using on-line gas chromatography (Perkin-Elmer: Clarus 580, MolSieve MS5A 25 x 0.53 and Pora Plot U 25 x 0.53 columns, TCD, FID, Ar carrier).

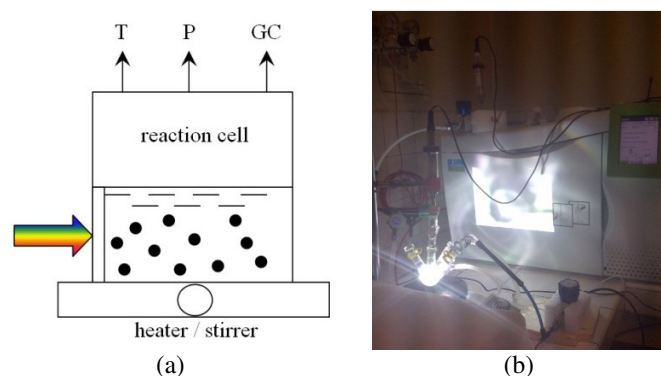


**Figure 1** (a) schematic diagram and (b) photograph of the experimental setup used for experiments with Co co-catalyst.

### Exafs/xanes experiments

Exafs experiments for the characterization of the cobalt complex have been performed at the SOLEIL synchrotron radiation facility in France.

### METHANOL STEAM PHOTO-REFORMING USING RHODIUM-DOPED STRONTIUM TITANATE WITH Pt

The powder sample of rhodium-doped strontium titanate surface modified by deposition of platinum nanoparticles was dispersed in a water-methanol mixture to perform the endergonic methanol steam photo-reforming reaction at close-to-room temperature, under visible light irradiation.

### Photocatalytic activity for H<sub>2</sub> evolution under visible light irradiation [4]

Pt/SrTiO<sub>3</sub>:Rh(1%) photocatalyst showed high activity for H<sub>2</sub> evolution from an aqueous methanol solution under visible light irradiation (Figure 2). An induction period was observed at the early stage of the photocatalytic reaction. The induction period suggests that some reduction process should have proceeded at the beginning stage instead of water reduction. After purging the cell, a similar kinetic trend was observed. The rate of hydrogen evolution is a function of photo-material concentration and light intensity. In figure 2, the initial rate of  $\approx 80 \mu\text{mol H}_2 \text{ h}^{-1}$  tends to reach a lower steady state value of  $\approx 30 \mu\text{mol H}_2 \text{ h}^{-1}$  within a few hours. A maximum rate of  $117 \mu\text{mol H}_2 \text{ h}^{-1}$  has been measured on fresh samples.

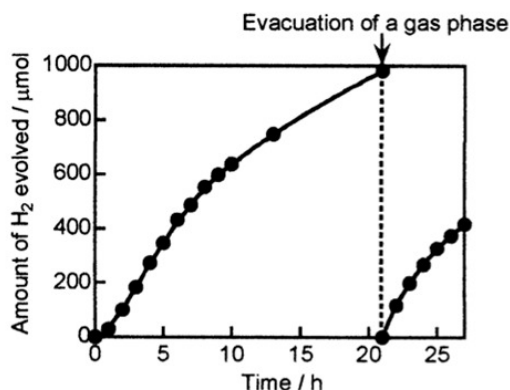


**Figure 2** H<sub>2</sub> evolution from an aqueous methanol solution under visible light irradiation over a Pt/SrTiO<sub>3</sub>:Rh photocatalyst.

### Band structure of SrTiO<sub>3</sub>:Rh and mechanism of photocatalytic H<sub>2</sub> evolution [4, 7-8]

Band structure and the schematic mechanism for the photocatalytic H<sub>2</sub> evolution on Pt/SrTiO<sub>3</sub>:Rh are illustrated in Figure 3. The visible light absorption bands in the diffuse reflectance spectrum suggested the existence of at least two different Rh species in the doped material. They can be assigned to be Rh<sup>3+</sup> and a rhodium species with a higher oxidation number than Rh<sup>3+</sup> such as Rh<sup>4+</sup>. The Rh with the higher oxidation number can be easily reduced to Rh<sup>3+</sup> by photogenerated electrons at the early stage of the photocatalytic reaction, indicating the Rh with the higher oxidation number works as an electron acceptor. The highly efficient H<sub>2</sub> evolution on the SrTiO<sub>3</sub>:Rh photocatalyst under visible light irradiation indicates that Rh<sup>3+</sup> works as an electron donor. The absorption band remaining after the reduction by photogenerated electrons should be the transition from the donor level formed with Rh<sup>3+</sup> to the conduction band. This is the key process for the photocatalytic H<sub>2</sub> evolution on Pt/SrTiO<sub>3</sub>:Rh under visible light irradiation. Electrons photogenerated in the conduction band reduce water to form H<sub>2</sub> while holes formed in the electron donor level possessed thermodynamic and kinetic potentials for oxidation of methanol. This is an indication that the doped Rh<sup>3+</sup> formed the visible light absorption center and the surface reaction center. The band structure was also confirmed by DFT calculation, X-ray absorption spectroscopy, and X-ray emission spectroscopy.

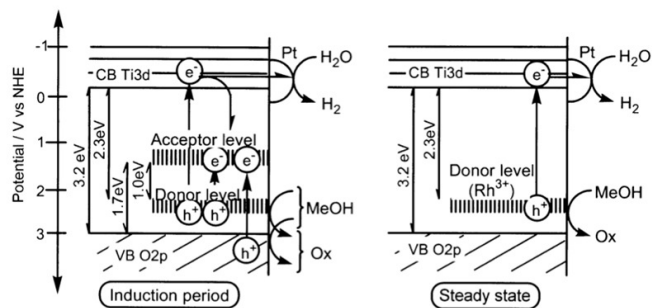


**Figure 3** Band structure and visible light response of SrTiO<sub>3</sub>:Rh photocatalyst.

### Photoelectrochemical Property of SrTiO<sub>3</sub>:Rh [9]

Figure 4 shows photo-response in the current-potential curves of SrTiO<sub>3</sub> and SrTiO<sub>3</sub>:Rh(1 atom%) electrodes. SrTiO<sub>3</sub> gave anodic photocurrent under only UV irradiation indicating an n-type character as reported. In contrast, the SrTiO<sub>3</sub>:Rh(1 atom%) electrode showed cathodic photocurrent with an onset potential at 0.6 V vs. a Ag/AgCl reference electrode. This result suggested that the SrTiO<sub>3</sub>:Rh(1 atom%) electrode possessed a p-type character. The photocurrent was confirmed to be due to water splitting by analyzing evolved H<sub>2</sub> and O<sub>2</sub>. The water splitting proceeded by applying an external bias smaller than 1.23 V vs. a counter Pt electrode under visible light irradiation and also using a solar simulator, indicating that photoelectrochemical water splitting is possible using this material.

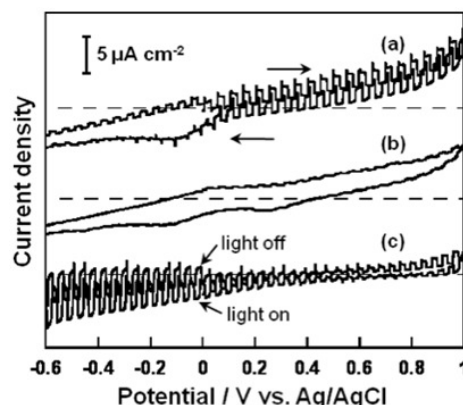


**Figure 4** Current vs. potential curves of (a) SrTiO<sub>3</sub> ( $\lambda > 300$  nm), (b) SrTiO<sub>3</sub> ( $\lambda > 420$  nm), and (c) SrTiO<sub>3</sub>:Rh ( $\lambda > 420$  nm) electrodes.

### Methanol oxidation products

Reaction products have been analyzed by gas chromatography, using two detectors, a flame ionization detector (FID) and a thermal conduction detector (TCD). Figure 5 shows that in addition to hydrogen and carbon dioxide, the reaction also leads to the formation of several carbonaceous species such as methane (ethylene and ethane were also detected). However, no carbon monoxide was detected. These species are by-products of either methanol oxidation or decomposition or reduction. The main broad peak observed between 5 and 20 minutes (not represented here) is due to the water-methanol mixture. The hydrogen to carbon ratio was found to be approximately 3, corresponding to the stoichiometry of reaction (3). However, the detection of methane and ethane (the carbon oxidation level of which is lower than that of methanol, table 1), suggests that multiple reaction paths are taking place, a situation that will require further investigations.

Species	CH <sub>3</sub> OH	CO <sub>2</sub>	CH <sub>4</sub>	C <sub>2</sub> H <sub>4</sub>	C <sub>2</sub> H <sub>6</sub>
degree	-II	+IV	-IV	-II	-III

**Table 1** : oxidation state of carbonaceous reaction products

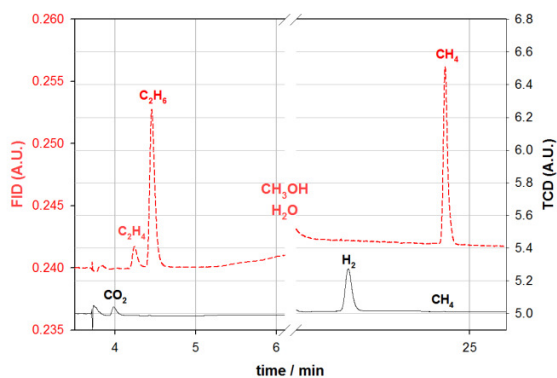


**Figure 5:** gas chromatograms showing the increasing concentration of species with time.

## METHANOL STEAM PHOTO-REFORMING USING THE COBALT CO-CATALYST

The rate of water photo-reduction on pristine SrTiO<sub>3</sub>:Rh samples is very low. This is an indication that the material has very limited intrinsic activity towards the two half-reactions (1) and (2) mentioned above. As discussed in the previous section, the kinetics of the reaction is increased by surface deposition of metallic platinum nano-particles that act as surface co-catalyst. This is a clear indication that charge transfer processes at the semi-conductor/electrolyte interface can be considered (at least partly) as rate-determining, a situation that requires additional investigations. Hence, our interest for surface co-catalysis has been extended to surface grafting of molecular compounds and we report here on preliminary results obtained with a cobalt-clathrochelate that is known to be efficient electrocatalysts for the hydrogen evolution reaction during water electrolysis [5,10-11].

### Structural characterization

Figure 6-a shows the general structure of cobalt tris-glyoximate (clathrochelates) compounds.

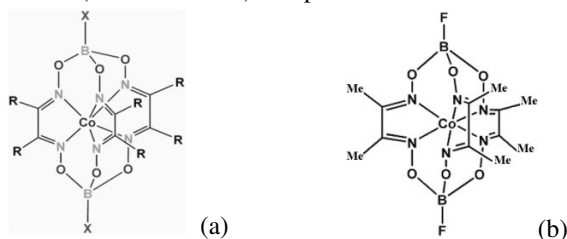


**Figure 6** (a) general structures of cobalt clathrochelates; (b) structure of the cobalt dimethyl tris-glyoximate.

This is a family of boron-capped tris(glyoximate) complexes. The metal active centre is covalently bounded to a shield of organic ligands that are selected and used for different purposes: (i) to prevent Co dissolution at rest potential conditions (the Co<sup>II</sup> species stable at rest potential does not dissolve in the electrolyte); (ii) to tune the redox potential of the active centre to the potential of interest (0 Volt versus RHE for the hydrogen evolution reaction or HER); (iii) to covalently

bond the complex to the surface of carbonaceous substrates used as electronic carriers in catalytic layers. Results reported in this communication have been obtained using dimethyl and diphenyl tris-glyoximates.

### Electrochemical characterization

Figure 7 shows the cyclic voltamograms of the two species recorded at a glassy carbon working electrode in acetonitrile (ACN). The first one (figure 7-a) is the cobalt dimethyl tris-glyoximate [Co(dmg)<sub>3</sub>(BF)<sub>2</sub>]<sup>+</sup>. The second one (figure 7-b) is the cobalt diphenyl tris-glyoximate [Co(dpg)<sub>3</sub>(BF)<sub>2</sub>]<sup>+</sup>. These two complexes display similar reversible waves corresponding to the Co<sup>III</sup>/Co<sup>II</sup> and Co<sup>II</sup>/Co<sup>I</sup> redox couples. The electronic properties of the central cobalt active centre are significantly modulated by the chemical environment. Chemical radicals located on the glyoximate ligands can induce significant electronic effects. Electronic acceptor effects tend to shift the cyclic voltamograms along the potential axis towards higher potential values of higher energy. For example, the replacement of methyl radicals by phenyl ones shifts the half-waves of the Co<sup>II</sup>/Co<sup>I</sup> redox couple by ≈ 250 mV upwards. Both complexes are stable up to +1.0 V/SCE, a value higher than the potential of the methanol/CO<sub>2</sub> redox couple.

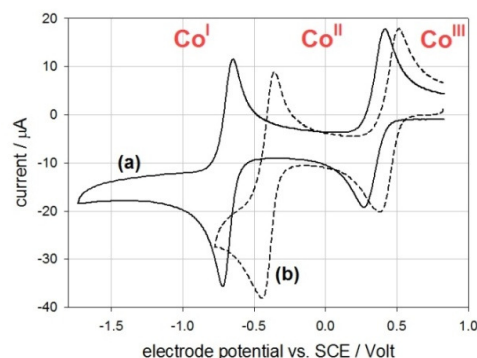


**Figure 7** Cyclic voltamograms measured on (a) [Co(dmg)<sub>3</sub>(BF)<sub>2</sub>]<sup>+</sup> and (b) [Co(dpg)<sub>3</sub>(BF)<sub>2</sub>]<sup>+</sup> in ACN + n-Bu<sub>4</sub>NClO<sub>4</sub> 4 mM (at 25°C, 50 mV/s).

The electrochemical activity of these complexes with regard to the HER has already been reported [5]. It can be put into evidence by adding increasing amounts of protons to the solution. As the proton to cobalt ratio is increased, a reduction current of increasing intensity (due to the hydrogen evolution reaction), is observed (figure 8). Proton reduction into molecular hydrogen is triggered by the formation of the Co<sup>I</sup> species which is prone to form Co hydrides and plays a role in the reduction mechanism. A proper selection of radicals (R- in Fig. 6-a) is required to tune the half-wave potential of the Co<sup>II</sup>/Co<sup>I</sup> species and to shift the reduction potential as close as possible to the standard potential of the H<sup>+</sup>/H<sub>2</sub> redox couple, and even above if possible. Depending on the chemical composition of the complex that is used, the HER is more or less efficient. Experiments show that these complexes are stable over significantly long periods of time [12].



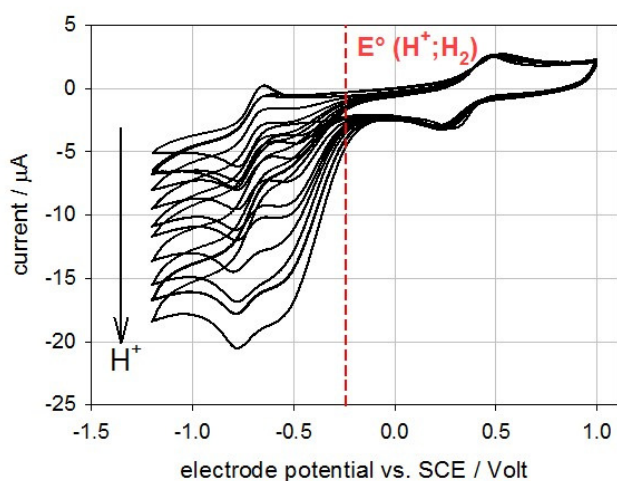


**Figure 8** Cyclic voltammograms measured on glassy carbon in a 0.2 mM solution of  $[\text{Co}(\text{dmg})_3(\text{BF}_2)_2]^+$  in ACN +  $n\text{-Bu}_4\text{NClO}_4$  4 mM (25°C, 50 mV/s) with increasing  $\text{H}^+/\text{Co}$  ratio.

#### Exafs/xanes characterization

The cobalt dimethyl tris-glyoximate complex of figure 6-b has been characterized using exafs spectroscopy. Figure 9 shows results obtained at the Co K-edge. Spectrum (a) was obtained with the complex in powder form; spectrum (b) was obtained with the complex in solution in DMF; spectrum (c) was obtained with the complex in solution in DMF after chemical reduction by  $\text{NaBH}_4$ . Whereas edge features of the sample either in solid form or in solution are very close, significant differences are observed with the complex in its reduced form ( $\text{Co}^{\text{I}}$  species): (i) the edge features, and (ii) the number and shape of oscillations that follow the first absorbance maximum are both different. The edge position (the energy of the inflection point in the rise at the edge) and threshold peak height are related to the electron density near the absorbing atom. The edge position moves to higher energy and the relative threshold peak height increases as the metal becomes electron deficient, *i.e.*, is oxidized or undergoes perturbation of the valence orbitals by ligands [13].

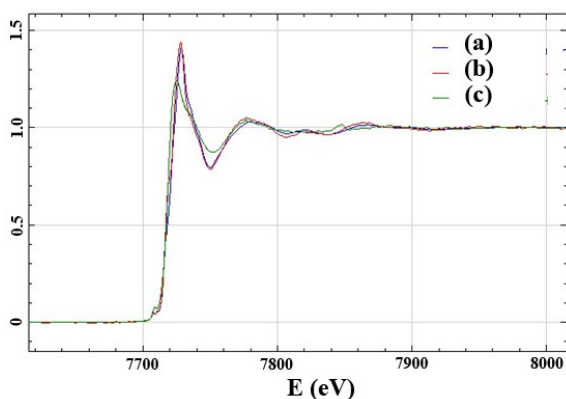


**Figure 9** Co K-edge XANES spectra of the Co dimethyl tris-glyoximate shown in figure 5-b. (a) powder; (b) in solution in DMF; (c) in solution in DMF after reduction by  $\text{NaBH}_4$ .

Figure 10 shows the radial distributions  $X(R)$  corresponding to the three XANES spectra (a = powder, b = solution in DMF, c = reduced Co species) of figure 9. For the solid and for the complex in solution, the first peaks at approximately 1.35 Å are due to the Co-N first shell contribution, while the next peaks between 2.00 and 3.00 Å are essentially due to the Co-O contribution. A comparison of spectra (a) and (b) shows that in solution, the first N shell is slightly shifted toward longer distances, an expansion that can be attributed to limited solvation effects, due to the aprotic polar DMF molecules. Spectrum (c) is that of the reduced  $\text{Co}^{\text{I}}$  species which is significantly different from the spectrum of metallic cobalt. However, a comparison of spectra (a) and (b) with spectrum (c) reveals that in the reduced form, the first shell is not significantly impacted by the reduction. This is the confirmation that the glyoximate ligand shield is chemically stable, as already suggested by the reversibility of the cyclic voltammogram shown in figure 7.

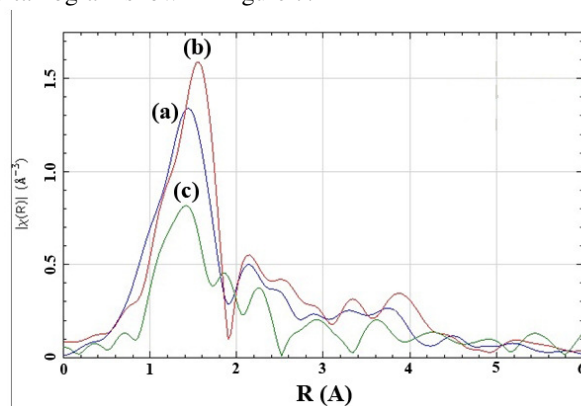


**Figure 10** Fourier-transforms of the experimental EXAFS spectra of figure 9.

#### Kinetics of methanol photo-reforming

We report here on preliminary results obtained with  $\text{SrTiO}_3:\text{Rh}$  and cobalt clathrochelates as molecular co-catalysts, using the experimental setup of figure 1. Results are plotted in figure 11. Data points of curves (a), (b) and (c) were obtained using  $\approx 10 \text{ cm}^3$  of  $\text{Pt-SrTiO}_3:\text{Rh}$  (1 wt.%) in the water-methanol solution, at different concentrations, and a light source of  $\approx 40 \text{ mW/cm}^2$ . The same general trend as that of figure 2 is observed, but smaller rates (from initially  $\approx 0.1$  up to  $\approx 0.6 \mu\text{mol H}_2 \text{ h}^{-1}$  when the steady state is reached) are obtained. This is due to the lesser amount of photo-active material and the different power source. It is also observed that the  $\text{H}_2$  production rate tends to increase when the concentration (expressed in  $\text{mg}\cdot\text{cm}^{-3}$ ) of perovskite is decreased: when the solution with the suspension of photoactive powder is too concentrated, light cannot illuminate the entire volume of the reactor and only a fraction of perovskite particles are active.

Curve (d) was obtained using a water methanol solution of  $2 \text{ mg/cm}^3$   $\text{SrTiO}_3:\text{Rh}$  (1wt.%) and  $1 \text{ mg/cm}^3$  of the cobalt dimethyl tris-glyoximate  $[\text{Co}(\text{dmg})_3(\text{BF}_2)_2]^+$  of figure 6-b. Although the solubility of the complex in water is limited, its solubility in the water-methanol mixture was sufficient for the experiment.

After introduction of the complex, the colour of the solution immediately turned to brownish-red. During the first hours of the experiments, the kinetics of the reaction had a similar trend to those measured on the Pt-SrTiO<sub>3</sub>:Rh(1wt.%) samples, although the rate of evolving hydrogen was lower. Since a co-catalyst is required for both water reduction and methanol oxidation, and since the cobalt complex has no specific activity with regard to methanol oxidation, this may explain the reduced reaction rate. After 4 hours of operation, a loss of activity has been observed. This can be attributed to either the inhibition of methanol oxidation or to surface contamination by Co-complex photo-degradation products (e.g. resulting from the interactions of surface oxidative holes with complexes) but additional investigations are required to clarify the point.

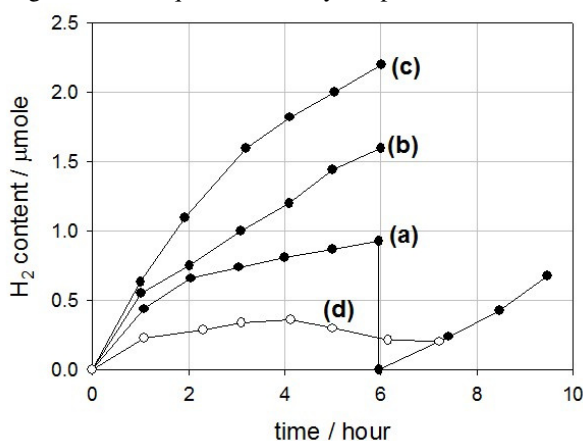


**Figure 11** H<sub>2</sub> evolution from an aqueous methanol solution under visible light irradiation using Pt-SrTiO<sub>3</sub>:Rh photocatalyst. (a) 3.58 mg/cm<sup>3</sup>; (b) 2.38 mg/cm<sup>3</sup>; (c) 1.93 mg/cm<sup>3</sup>. Curve (d) results obtained using the Co-SrTiO<sub>3</sub>:Rh photocatalyst.

## CONCLUSION

The purpose of this communication is to report on the photo-dissociation of water using Rhodium-doped Strontium Titanate surface modified by deposition/adsorption of co-catalysts and methanol as sacrificial agent. The rate of the photo-reaction has been measured by gas chromatography analysis. Negligible amounts of hydrogen and carbon dioxide were found to form on pristine samples. It is shown that the kinetics and efficiency of the photo-reduction process is favored by surface deposition of platinum nanoparticles. This is an indication that charge transfer processes at the semiconductor/electrolyte interface can be considered (at least partly) as rate-determining. Our interest for surface co-catalysis has been extended to surface grafting of molecular properties and we report here preliminary results obtained by surface addition of some cobalt-clathrochelates that are known to be efficient electrocatalysts for the hydrogen evolution reaction during water electrolysis. It is found that the presence of cobalt complexes has also a positive catalytic effect on the kinetics of the reaction but an overall loss of performance has been observed with time. This can be attributed to either inhibition of methanol oxidation or to surface contamination by Co-complex photo-degradation products.

In terms of perspectives, several still unanswered questions need to be addressed. First we plan to further investigate the role of cobalt complexes on pristine SrTiO<sub>3</sub>:Rh powder by coating the powder sample onto a FTO substrate electrode to form a photo-electrode that could facilitate electrochemical experiments. Second, we plan to investigate the nature of interactions between the semi-conductor and the Co-complexes since surface functionalization is critical to design efficient structures. Finally, we plan to perform experiments with clathrochelate complexes of different chemical composition to identify the most efficient ones for the reaction of interest.

## REFERENCES

- [1] Bak T., Nowotny J., Rekas M., Sorrell C.C., Photo-electrochemical hydrogen generation from water using solar energy. Materials-related aspects, *International Journal of Hydrogen Energy*, Vol. 27, 2002, pp. 991-1022
- [2] Fujishima A., Honda K., Electrochemical Photolysis of Water at a Semiconductor Electrode, *Nature*, Vol. 238, 1972, pp. 37-38.
- [3] Kudo A., Miseki M., Heterogeneous photocatalyst materials for water splitting, *Chem. Soc. Rev.*, Vol. 38, 2009, pp. 253-278.
- [4] Kouta R., Ishii T., Kato H., Kudo A., Photocatalytic activities of noble metal ion doped SrTiO<sub>3</sub> under visible light irradiation, *J. Phys. Chem. B.*, Vol. 108, 2004, pp. 8992-8995.
- [5] Dinh Nguyen M-T., Ranjbari A., Catala L., Brisset F., Millet P. and Aukauloo A., Implementing Molecular Catalysts for Hydrogen Production in Proton Exchange Membrane Water Electrolysers, *Coord. Chem. Review*, Vol. 256, 2012, pp. 2435-2444
- [6] Jackels S.C., Zektzer J., Rose N. J., Goeken V.L., and Chapman R., in *Inorganic Syntheses*, McDiarmid A. G. Ed., McGraw-Hill, Vol. 17, 1977, pp 139-147
- [7] Kawasaki S., Akagi K., Nakatsuji K., Yamamoto S., Matsuda I., Harada Y., Yoshinobu J., Komori F., Takahashi R., Lippmaa M., Sakai C., Niwa H., Oshima M., Iwashina K., and Kudo A., Elucidation of Rh-Induced In-Gap States of Rh:SrTiO<sub>3</sub> Visible-Light-Driven Photocatalyst by Soft X-ray Spectroscopy and First-Principles Calculations, *J. Phys. Chem. C*, Vol. 116, 2012, pp. 24445-24448.
- [8] Kawasaki S., Nakatsuji K., Yoshinobu J., Komori F., Takahashi R., Lippmaa M., Mase K., and Kudo A., Epitaxial Rh-doped SrTiO<sub>3</sub> thin film photocathode for water splitting under visible light irradiation, *Appl. Phys. Lett.*, Vol. 101, 2012, pp. 033910(1-4).
- [9] Iwashina K. and Kudo A., Rh-doped SrTiO<sub>3</sub> photocatalyst electrode showing cathodic photocurrent for water splitting under visible-light irradiation, *J. Am. Chem. Soc.*, Vol. 133, 2011, pp. 13272-13275.
- [10] Pantani O., Anxolabéhère E., Aukauloo A., Millet P., Electroactivity of cobalt and nickel glyoximes with regard to the electro-reduction of protons into molecular hydrogen in acidic media, *Electrochem. Commun.*, Vol. 9, 2007, pp. 54-58
- [11] Pantani O., Naskar S., Guillot R., Millet P., Anxolabéhère E., and Aukauloo A., Cobalt Clathrochelate Complexes as Hydrogen-Producing Catalysts, *Angewandte Chemie Int. Ed.*, Vol. 120, 2008, pp. 10096-10098
- [12] Millet P., Rozain C., Villagra A., Ragupathy A., Ranjbari A. and Guymont M., Implementation of cobalt clathrochelates in polymer electrolyte water electrolysers for hydrogen evolution, *Chem. Engineering. Trans.*, Vol. 41, 2014, DOI:10.3303/CET1441055
- [13] Weber R. S., Peuckert M., DallaBetta R. A., and Boudart M., Oxygen Reduction on Small Supported Platinum Particles: II. Characterization by X-ray Absorption Spectroscopy, *J. Electrochem. Soc.*, Vol. 135, 1988, pp. 2535-2538.